

Supporting Information for

Binder effect on oxide-based anode in lithium and sodium-ion battery

applications: the fastest way to ultrahigh performance

Jun Ming,^{a‡} Hai Ming,^{ab‡} Won-Jin Kwak,^a Changdae Shin,^a Junwei Zheng,^b Yang-

Kook Sun^{a*}

^a *Department of Energy Engineering, Hanyang University, Seoul 133-791, South Korea*

^b *College of Chemistry, Chemical Engineering and Materials Science, Soochow University, Suzhou 215123, P. R. China*

Materials and Characterization

Materials synthesis

The metal oxides, include Co_3O_4 , CuO , NiO and Fe_2O_3 , were obtained *via* calcination of corresponding metal nitrate of $\text{Co}(\text{NO}_3)_2 \cdot 6\text{H}_2\text{O}$, $\text{Cu}(\text{NO}_3)_2 \cdot 6\text{H}_2\text{O}$, $\text{Ni}(\text{NO}_3)_2 \cdot 6\text{H}_2\text{O}$ and $\text{Fe}(\text{NO}_3)_3 \cdot 6\text{H}_2\text{O}$ in furnace at 500 °C for 2 hours (heating rate, 5 °C min^{-1}) under the atmosphere of air. The as-prepared Fe_2O_3 and NiO powders were ball milled with carbon (acetylene black, AB) simply for 5 hours respectively with a mass ratio of 9:1, giving rise to $\text{Fe}_2\text{O}_3\text{-C}$ and NiO-C . The TiO_2 powders was prepared via the ways of hydrolyzing tetrabutyl titanate in the mixture of ethanol and water for 10 hours firstly and then calcination the dried powders of $\text{Ti}(\text{OH})_4$ in air at 450 °C for 5 hours (heating rate, 5 °C min^{-1}), finally giving rise to TiO_2 powders.

Electrode preparation

The sample of metal oxide, conductive material of acetylene black (AB) and binders of carboxymethyl cellulose (CMC), polyacrylic acid (PAA) with a mass ratio of 75:15:5:5 were mixed well with using water as solvent, and then the resultant uniform slurry was casted on the copper foil by the doctor blade. Subsequently, the electrode was completely dried at room temperature and then at 80 °C in vacuum oven overnight. Note that the composite binder of PAA/CMC is better than single PAA or CMC. Moreover, judged from the experimental phenomena, the binder of PAA could make the electrode to be casted more uniformly. Press the electrode by the rolling machine before punching to the circular electrode with a diameter of 14 mm ($\text{Ø}14$). The mass density of active materials of metal oxide (i.e., except the mass of AB and

binder) on copper foil was controlled accurately around 1.3 mg cm^{-2} .

Characterization

Crystallographic information of metal oxides were investigated by XRD, which were measured on a Bruker D8 GADDS diffractometer using Co K α radiation (1.79 \AA). The morphology and structure of metal oxide powders were characterized by field emission scanning electron microscopy (FESEM), which was taken on a XL30 ESEM microscope with a beam energy of 20 kV. The fourier transform infrared spectroscopy (FTIR) was processed in the N $_2$ filled glove box. The 2032-type coin cell was assembled in the glove box in which the water and oxygen content are both below 0.1 ppm. In the lithium ion battery test, the electrolyte was 1.2 M LiPF $_6$ in ethylene carbonate/ethylmethyl carbonate (EC/EMC) (v/v, 3/7) and polypropylene was used as the separator. While in the sodium ion battery, the used electrolyte was 1.0 M NaClO $_4$ in propylene Carbonate (PC) with 2vol.% fluoroethylene carbonate (FEC), and the glass fibre was used as separator. All the half cells of metal oxide-based electrode versus lithium or sodium metal were discharged/charged at the voltage of 0.01-3.0 V with using the instrument of *TOCAST* 3100 at the temperature of 30 °C.

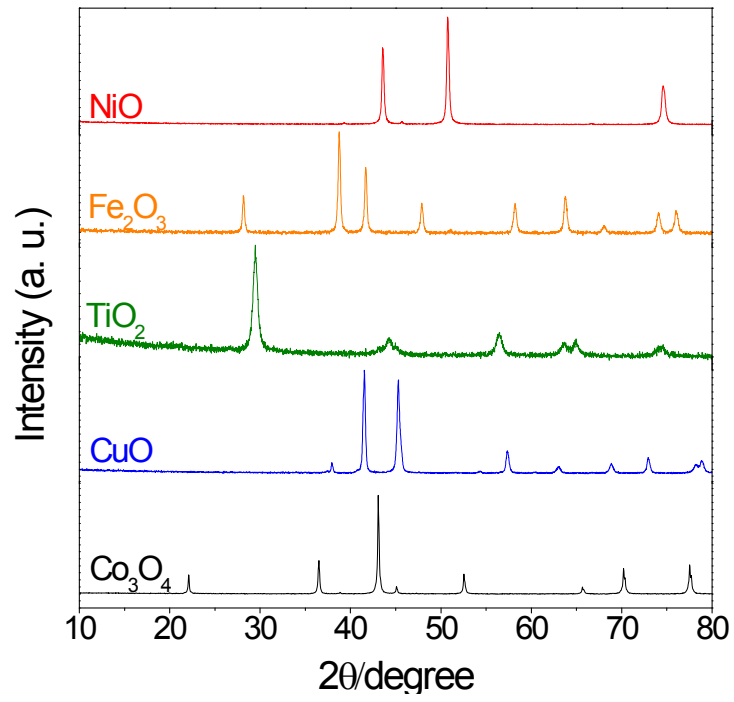


Figure S1 XRD patterns of metal oxide powders of Co_3O_4 , CuO , TiO_2 , Fe_2O_3 and NiO .

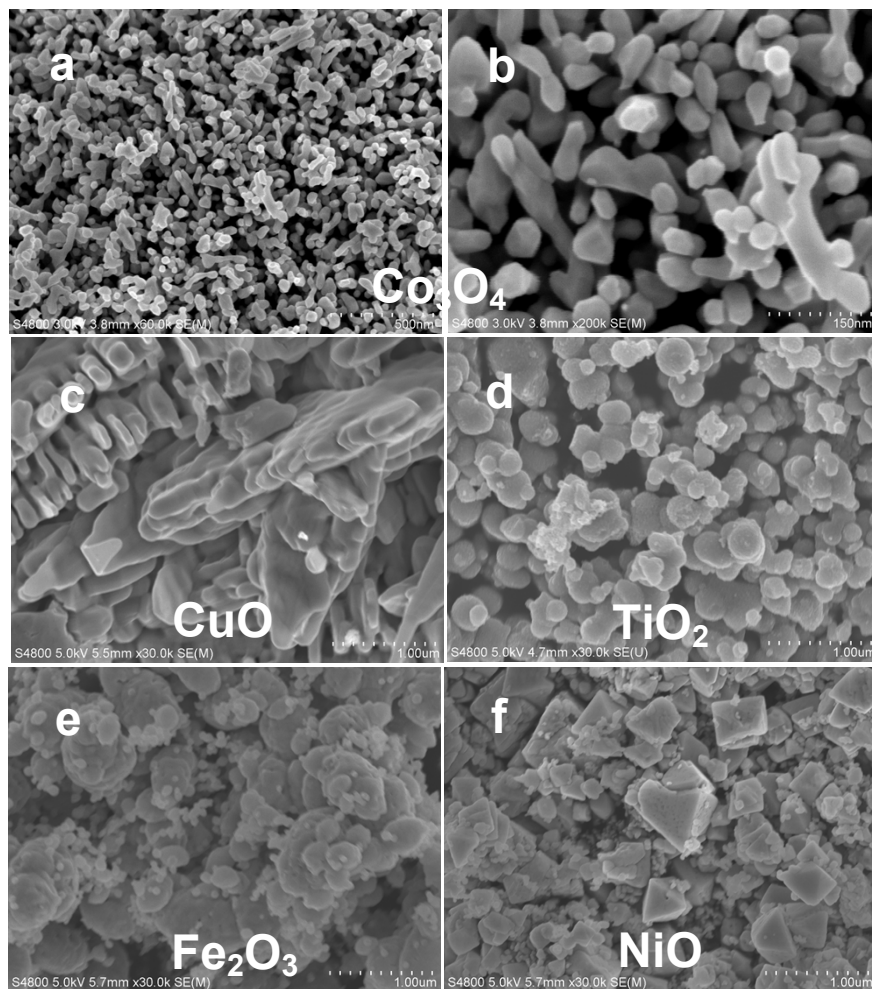


Figure S2 SEM images of metal oxide powders, (a, b) Co_3O_4 , (c) CuO , (d) TiO_2 , (e) Fe_2O_3 , (f) NiO .

Table S1 A detail compare of performances of metal oxides under the current density of 100 mA g⁻¹ with using different kind of binders.

Kind of metal oxide ^a	Co ₃ O ₄	CuO	TiO	Fe ₂ O ₃	NiO	Fe ₂ O ₃ -C ^b	NiO-C ^b
2							
PVDF							
Capacity (2 nd cycle)/mAhg ⁻¹	651	238	144	822	606	1038	746
Capacity (50 th cycle)/mAhg ⁻¹	518	324	149	177	425	758	615
Capacity retention (%)	79.6	136	103	21.5	70.1	73.0	82.4
PAA/CMC							
Capacity (2 nd cycle)/mAhg ⁻¹	1043	401	326	1018	762	1203	944
Capacity (90 th cycle)/mAhg ⁻¹	1311	630	409	712	695	1155	937
Capacity retention (%)	126	157	125	70.5	91.2	96.0	99.3

^aThe mass density of active materials of metal oxide on the copper electrode (i.e., except the mass of binders and AB) was controlled accurately around 1.30 mg cm⁻² for a rational compare.

^bThe data of Fe₂O₃-C and NiO-C electrode was obtained at 50 cycles, rather than 90 cycles in the case of using PAA/CMC as binders.

Table S2 A detail performance of metal oxide under the rate test ranging from 100, 250, 500, 1000, 2500 to 5000 mA g⁻¹ with using PAA/CMC as binder.

Kind of metal oxide	Current density / mA g ⁻¹						
	100	250	500	1000	2500	5000	100 (recover)
Co ₃ O ₄ ^a	1057	1065	1018	905	618	262	1171
CuO ^b	644	545	443	305	145	68	684
TiO ₂ ^b	428	402	370	307	236	160	462
Fe ₂ O ₃ -C ^a	1201	1140	996	583	119	43	1169
NiO-C ^a	964	936	859	542	139	52	947

^aThe New cell was assembled to confirm the reproducibility of the materials;

^bThe used cell after the cycling performance in figure 1b was continually tested in rate test for further demonstrating the stability and cycle ability of the materials.

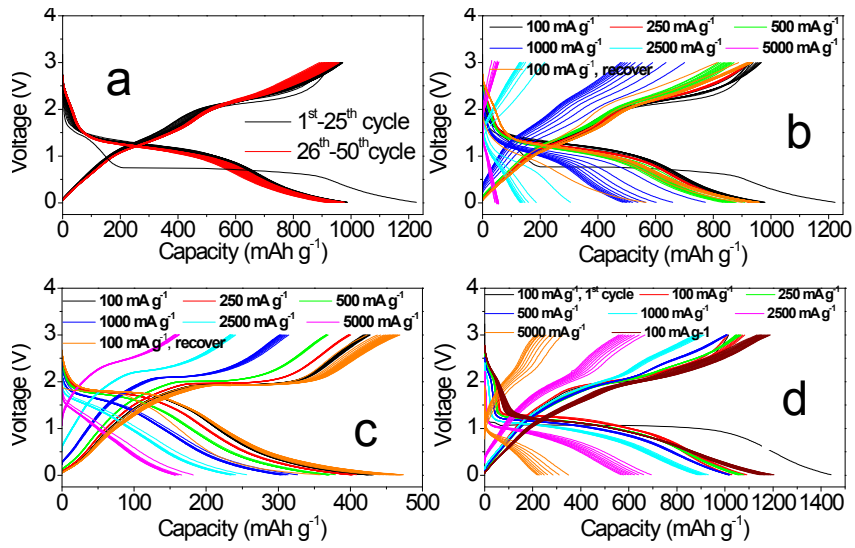


Figure S3 Typical charge-discharge curves of NiO-C-PAA/CMC in the (a) cycling and (b) rate test. Typical charge and discharge curves of (c) TiO₂-PAA/CMC (the used cell after cycling test) and (d) Co₃O₄-PAA/CMC (the new cell) in the rate test.

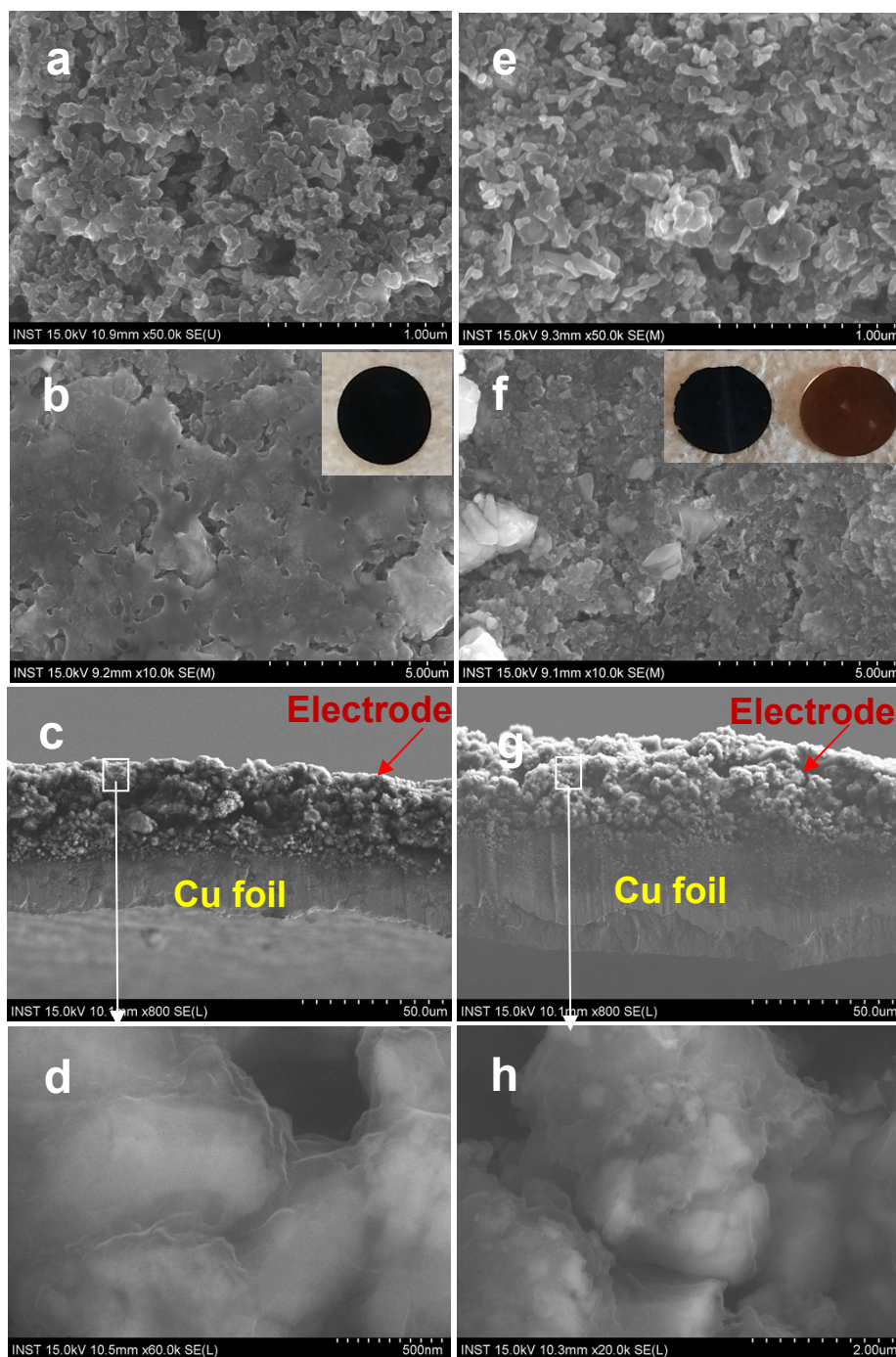


Figure S4 SEM and cross-section images of electrode of (a, b-d) Co_3O_4 -PAA/CMC and (e, f-h) Co_3O_4 -PVDF before and after cycling. Inset of (b) and (f) are typical comparative digital pictures of Co_3O_4 -PAA/CMC and Co_3O_4 -PVDF electrode after cycling. Most electrodes using PVDF as binder have the common phenomena of collapse and desperation from the copper foil after disassembling the cell. (d) and (h) are the high resolution SEM images of electrode of (c) and (g) respectively. After the cycling, the volume variation of (g, h) Co_3O_4 -PVDF was much larger and rougher than that of (c, d) Co_3O_4 -PAA/CMC, further demonstrating the weaker adhesion ability of PVDF and the higher stability of Co_3O_4 -PAA/CMC electrode .

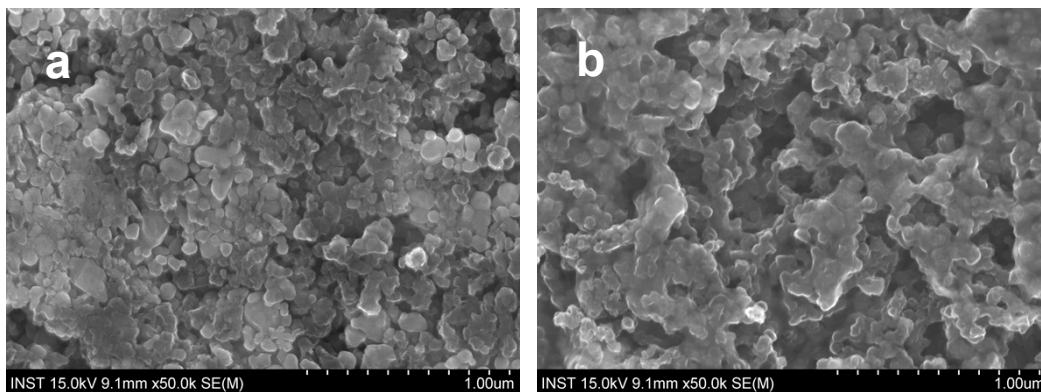


Figure S5 SEM images of pristine electrodes of (a) Fe₂O₃-PAA/CMC and (b) Fe₂O₃-C-PAA/CMC.

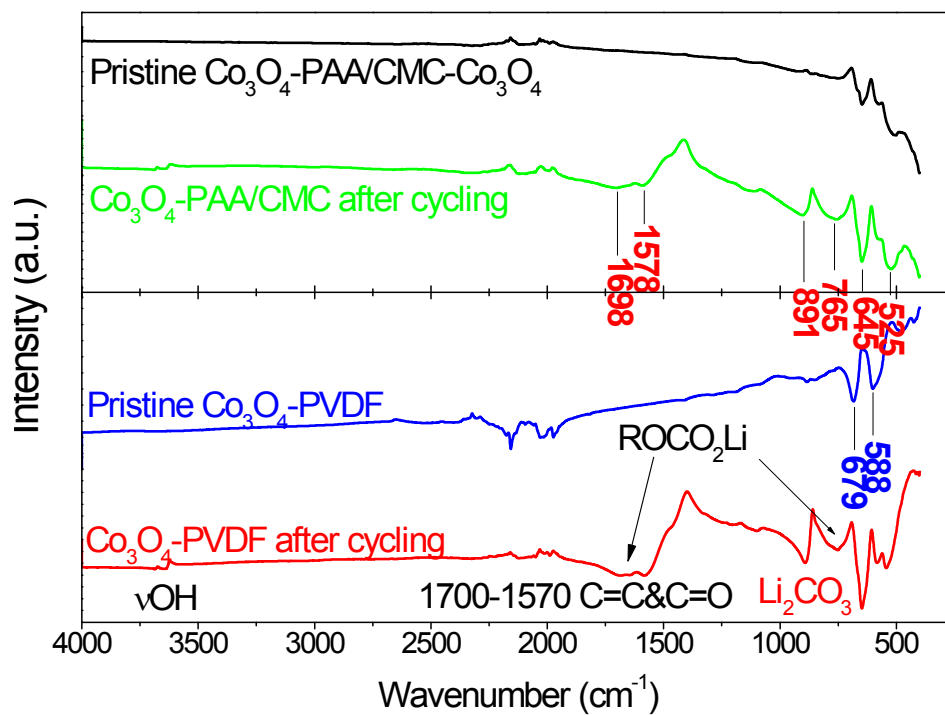


Figure S6 FTIR of Co_3O_4 -based electrodes with using different binders before and after cycling.

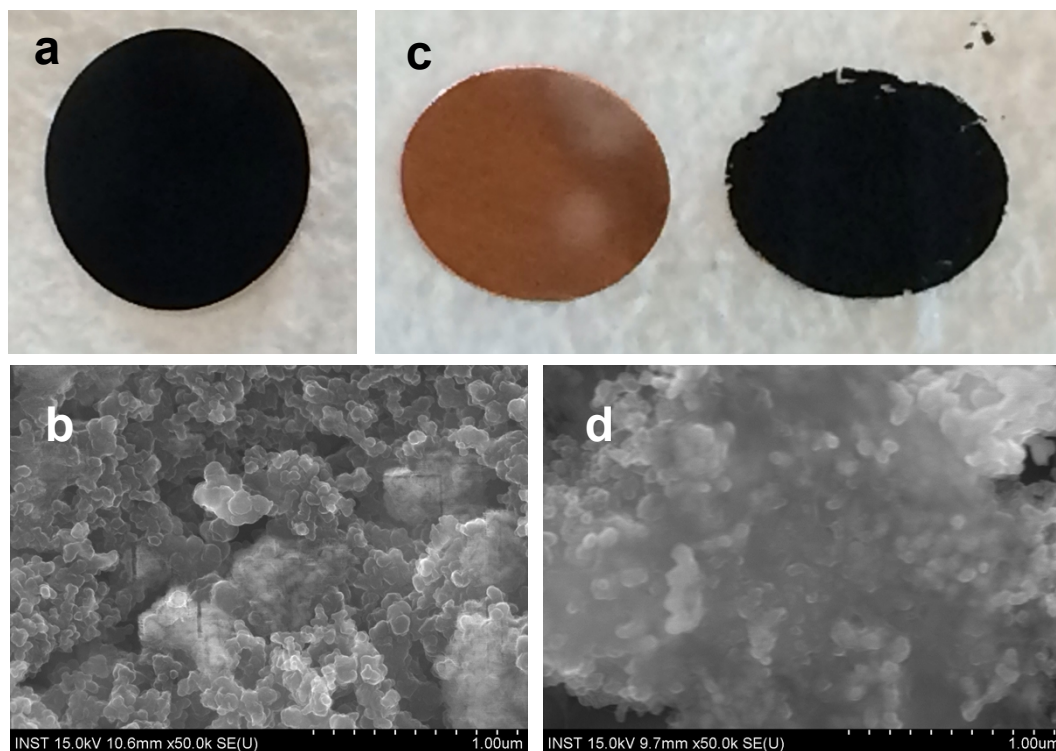


Figure S7 Typical comparative digital pictures and SEM images of (a, b) Co_3O_4 -PAA/CMC and (c, d) Co_3O_4 -PVDF after contacting with lithium metal for 10 min under the pressure of 50 g cm^{-2} . The electrode of Co_3O_4 -PVDF collapsed and was separated from the copper foil after the reaction, demonstrating the lower adhesion ability of PVDF. SEM images also directly showed the better endure ability of PAA/CMC binder in the expansion of metal oxide.

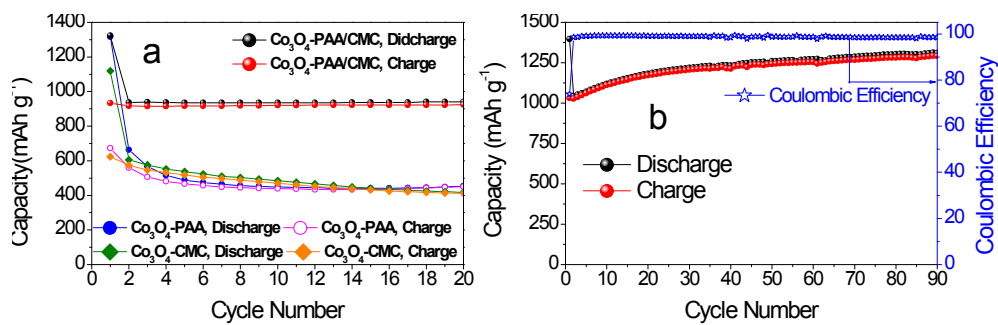


Figure S8 (a) Comparative electrochemical performance of Co₃O₄-based electrode with using PAA/CMC, PAA, CMC as binder respectively under the current density of 200 mA g⁻¹. (b) Coulombic efficiency of Co₃O₄-PAA/CMC electrode under the current density of 100 mA g⁻¹ in the initial 100 cycles.